Lagrangian Coherent Structures in magnetized plasmas: particle transport in a time dependent magnetic configuration

D. Grasso[1], G. Di Giannatale[2], M.V. Falessi[3], F. Pegoraro[4], T.J. Schep[5]

[1] *ISC - CNR and Politecnico di Torino, Dip. Energia C.so Duca degli Abruzzi 24, Torino. Italy*

[2] *IGI - CNR, Corso Stati Uniti 4, Padova, Italy*

[3] *ENEA, C. R. Frascati, Via E. Fermi 45, Frascati, Italy*

[4] *Dip. Fisica E. Fermi, Pisa University, largo Pontecorvo 3, Pisa, Italy*

[5] *Dep. Applied Physics, Eindhoven Univ. of Technology, 5600MB Eindhoven, The Netherlands*

Abstract

The concept of Lagrangian Coherent Structures (LCS) has been introduced by G. Haller in the context of transport processes in complex fluid flows [1]. LCS are a generalization of the dynamical structures observed in autonomous and periodic systems to temporally aperiodic flows. They separate the flow domain into macro-regions inside which fast mixing phenomena take place. Over the finite time span which characterizes the LCS these macro-regions do not exchange fluid elements and thus act as transport barriers. In two recent articles [2, 3], we have applied this conceptual framework to the study of particle transport in a magnetized plasma by referring to a simplified model that uses magnetic field lines as a proxy for particle trajectories and that allows us to consider explicitly a magnetic configuration evolving in time on timescales comparable to the particle transit time through the configuration.

Lagrangian Coherent Structures as maximal repulsion-attraction material lines

Consider a dynamical system in 2D phase space $x = (x,y)$ with flow map $\phi^t_{t_0}(x_0) = x(t,t_0,x_0)$. Two neighbouring points x_0 and $x_0 + \delta x_0$ evolve into x and $x + \delta x$ under the linearized map $\delta x = \nabla\phi^t_{t_0}\,\delta x_0$. Consider a curve $\gamma_0 = \{x_0 = r(s)\}$ and at each point $x_0 \in \gamma_0$ define the unit tangent and normal vectors e_0 and n_0. In the interval $[t_0,t]$ the system dynamics advects γ_0 into γ_t, $x_0 \in \gamma_0$ into $x_t \in \gamma_t$, the tangent vector e_0 into $e_t = \nabla\phi^t_{t_0}(x_0)\,e_0 \,/\, [e_0\,C^t_{t_0}(x_0)\,e_0]^{1/2}$, and the normal vector n_0 into $n_t = \left(\nabla\phi^{t_0}_t\right)^T n_0 \,/\, [n_0\,C^{-1}(x_0)\,n_0]^{1/2}$. Here ^{T} stands for transposed and $C^t_{t_0}(x_0) \equiv \left(\nabla\phi^t_{t_0}\right)^T \nabla\phi^t_{t_0}$ is the *Cauchy-Green strain tensor* which describes the deformation of an arbitrarily small circle of initial conditions (i.c.), centered in x_0 and $C^{-1}(x_0) = C^{t_0}_t(x_0)$ (time interval marks are suppressed unless explicitly needed). Let ξ_{max} and ξ_{min} be its two eigenvectors with positive eigenvalues λ_{max} and λ_{min}. The curves with tangent vector along ξ_{min} and, respectively, ξ_{max} are called *strain lines* of the Cauchy-Green tensor. The *repulsion ratio* $\rho^t_{t_0}(x_0,n_0)$ is defined (see Ref.[4, 5]) as the ratio at which points initially near $x_0 \in \gamma_0$**,** increase their distance

from the curve $[t_o,t]$: $\rho^t_{t_0}(x_0,n_0) = n_t\,\nabla\phi^t_{t_0}(x_0)\,n_0. = [n_0\,C^{-1}(x_0)\,n_0]^{-1/2} = [n_t\,C(x_0)\,n_t]^{1/2}$. Analogously the *contraction rate* $L^t_{t_0}(x_0)$ is proportional to the growth in time of the tangent vector $L(x_0,e_0) = [e_0\,C(x_0)\,e_0]^{1/2}$. A (hyperbolic) LCS over a finite time interval $[t_0,t_0+T]$ is defined as a material line along which the repulsion rate is pointwise maximal. This leads to the following definitions: a material line such that at each point: $\lambda_{min} < \lambda_{max}$, $\lambda_{max} > 1$, $e_0 = \xi_{min}$, $\xi_{max}\cdot\nabla\lambda_{max} = 0$ is called a repulsive Weak Lagrangian Coherent Structure (WLCS). A WLCS which satisfies the additional condition $\xi_{max}\cdot\nabla^2\lambda_{max}\cdot\xi_{max} < 0$ is called a repulsive Lagrangian Coherent Structure. Attractive LCS are defined as repulsive LCS of the backward time dynamics. In the case of a Hamiltonian dynamical system with one degree of freedom, such as that which describes magnetic field lines at a fixed time (see e.g., [6]), we have $\lambda_{min}\,\lambda_{max} = 1$.

Magnetic field configuration

Following the study of multiple helicity magnetic reconnection in Ref.[7] we write $\mathbf{B} = B_0\mathbf{e}_z + \nabla\psi(x,y,z,t)\times\mathbf{e}_z$, with $\psi(x,y,z,t) = 0.19\cos(x) + \hat{\psi}_1(x,t)\cos(k_{1y}y+k_{1z}z) + \hat{\psi}_2(x,t)\cos(k_{2y}y+k_{2z}z)$ in the domain $[-L_x,L_x]\times[-L_y,L_y]\times[-L_z,L_z]$ with $L_x=\pi$, $L_y=2\pi$, $L_z = 16\pi$ with $k_{1y} = k_{2y} = 2\pi/L_y$ and $k_{1z} = 0$ while $k_{2z} = 2\pi/L_z$. Periodicity is assumed in all three directions. The initial perturbations, $\hat{\psi}_1(x,0)$ and $\hat{\psi}_2(x,0)$, are localized at the resonant surfaces $x_1 = 0$ and $x_2 = 0.71$ respectively. At each fixed physical time t the magnetic flux function $\psi(x,y,z,t)$ plays the role of the Hamiltonian for the magnetic field lines with x and y canonical variables and z the magnetic Hamiltonian time ($MH-t$). The field line equations become $dx/dz = -\partial\psi/\partial y$ and $dy/dz = \partial\psi/\partial x$. Different "helicities" k_z/k_y are needed to make the Hamiltonian non integrable, i.e., to generate a chaotic magnetic configuration.

In the linear phase two independent island chains are formed at their resonant surfaces: as they expand and start to interact the dynamics of the magnetic configuration becomes nonlinear, higher order modes (mostly with the same initial helicities) are generated and regions where field lines are stochastic are formed and spread as reconnection evolves [7]. We will consider the normalized physical time ($NP-t$) interval $t = 415-425$ in which chaos, initially developed only on a local scale (at $t = 415$), starts to spread on a global scale (at $t = 425$).

First we consider the dynamical system obtained by taking a snapshot at a given $NP-t$ where the flux function $\psi(x,y,z,t=\bar{t})$ is the Hamiltonian and z is the $MH-t$. Since the configuration is periodic in z we adopt the Poincaré map technique and compare it with the LCS approach. In addition since $\psi(x,y,z,t=\bar{t}) = \psi(x,-y,-z,t=\bar{t})$ attractive LCSs are mirror images of the repulsive LCSs with respect to $y = 0$.

Subsequently, in order to account for the magnetic configuration change during the particle transit time we adopt a simplified model where the particle gyromotion and drifts are neglected

and the particles dynamics is only included through their (constant) streaming velocity V along the guide field B_0. This allows us to describe LCSs in a time nonperiodic dynamical system and to identify LCSs that depend explicitly on the different particle velocities. Thus we introduce a family of nonautonomous dynamical systems characterized by a different velocity V, with Hamiltonian $\psi_V(x,y,z) \equiv \psi(x,y,z,t=(z-z_o)/V)$. Here $V>0$ is assumed, for negative V and for the modified relationship between repulsive and attractive LCSs see Ref.[2].

Numerical results

We find the hyperbolic LCSs, using the tool developed in Ref.[8]. Details of the application and optimization of this procedure to the present configuration and the criteria adopted in order to select the most relevant LCSs so as to produce a clear physical picture are given in Ref.[3].

MH-t periodic results

In left panel of Fig. 1 the LCS in the magnetic configuration at $NP-t=415$ are over plotted on the corresponding Poincaré map. The repelling (attractive) structures are drawn in red (blue). In this small amplitude phase the two perturbations with different helicities evolve independently from each other and each of them induces a magnetic island chain around its resonant surface. The right panel of Fig. 1 shows how the drawn LCS act as barriers for i.c. initially located where the green arrow points. These particles tend to align along the LCS without crossing it.

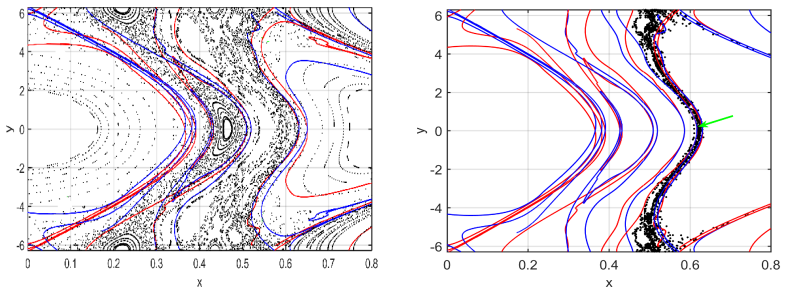

Figure 1: In the left panel the most important LCS are overplotted on the Poincaré map at $z=0$ and $t=415$. The repelling (attractive) structures are drawn in red (blue). In the right panel it is shown that i.c. located where the green arrow points cannot cross the barrier.

MH-t non periodic results

In Fig. 2 is shown the position at $t=415.2$ and $t=417$, in the left and right panel respectively, of two sets of i.c. initially separated by a LCS. In the left panel the two set of i.c. increase their distance exponentially, positioning themselves in such a way as to maximize their stretching in the perpendicular direction with respect to the LCS. In the right panel, it is clear that they obey different dynamics. The black i.c. have a chaotic behavior which distribute them along all the domain, while the green i.c. remain together, being influenced by the attractive nearby structure.

An important result is related to the fact that particles having different velocities see different transport barriers. In Fig. 3 the attracting LCS computed for particles having $V = 1000$ are shown in both panels. In the left (right) panel the positions of several sets of particles, initially located in different positions of the domain and having $V = 1000$ ($V = 200$) are overplotted. We observe that, although the particle positions for $V = 200$ appear qualitatively similar to those in left panel, they are shifted towards higher x-values with respect to black particles having $V = 1000$. This is due to the fact that particles having $V = 200$ see a stronger chaos (respect to particles with $V = 1000$) that decreases the regular area of the $m = 2$ island chain.

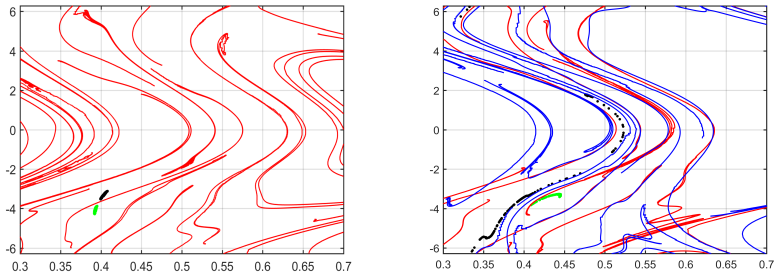

Figure 2: Position of i.c. separated by a LCS at $t = 415.2$ (417) on the left (right) panel.

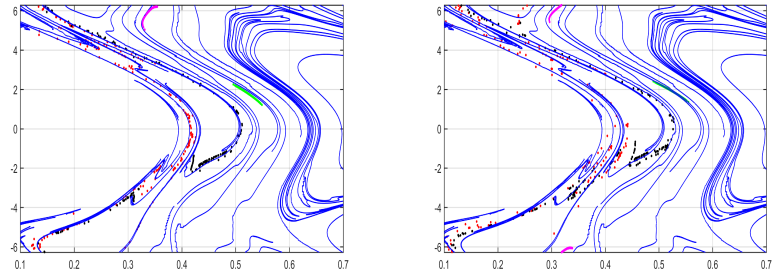

Figure 3: In the left (right) panel the position of different sets of i.c. evolved with $V = 1000$ ($V = 200$) overplotted on the LCS evaluated for $V = 1000$.

Conclusions and remarks

Lagrangian Coherent Structures provide a very convenient tool in order to identify in a compact and easily visualizable way the main features of the dynamics of the physical system under consideration as they provide a framework and a language to be used in characterizing the evolution of such features in time.

References

[1] G. Haller, *Annual Review of Fluid Mechanics,* **47** 137 (2015).

[2] G. Di Giannatale, M.V. Falessi, D. Grasso, F. Pegoraro, T.J. Schep, *Physics of Plasmas* **25**, 052306 (2018).

[3] G. Di Giannatale, M.V. Falessi, D. Grasso, F. Pegoraro, T.J. Schep, *Physics of Plasmas***25**, 052307 (2018).

[4] G. Haller, G. Yuan, *Physica D: Nonlinear Phenomena*. **147**, 352 (2000).

[5] M. V. Falessi, F. Pegoraro, T. J. Schep, *Journal of Plasma Physics*. **81**, 05 (2015)

[6] A. H. Boozer, *Physics of Fluids*, **24**, 1999 (1981).

[7] D. Borgogno, *et al. Physics of Plasmas*, **12**, 032309 (2005).

[8] K. Onu, F. Huhn, G. Haller, *Journal of Computational Science*, **7**, 26 (2015).